

## Laser micromachined hybrid open/paper microfluidic chips

B. Chumo, M. Muluneh, and D. Issadore<sup>a)</sup>

*School of Engineering and Applied Science, University of Pennsylvania,  
210 South 33rd Street, Suite 240 Skirkanich Hall, Philadelphia,  
Pennsylvania 19104-6321, USA*

(Received 17 September 2013; accepted 22 November 2013; published online 4 December 2013)

Paper-based microfluidics are an increasingly popular alternative to devices with conventional open channel geometries. The low cost of fabrication and the absence of external instrumentation needed to drive paper microchannels make them especially well suited for medical diagnostics in resource-limited settings. Despite the advantages of paper microfluidics, many assays performed using conventional open channel microfluidics are challenging to translate onto paper, such as bead, emulsion, and cell-based assays. To overcome this challenge, we have developed a hybrid open-channel/paper channel microfluidic device. In this design, wick-driven paper channels control the flow rates within conventional microfluidics. We fabricate these hybrid chips using laser-micromachined polymer sheets and filter paper. In contrast to previous efforts that utilized external, macroscopic paper-based pumps, we integrated micro-scale paper and open channels onto a single chip to control multiple open channels and control complex laminar flow-pattern within individual channels. We demonstrated that flow patterns within the open channels can be quantitatively controlled by modulating the geometry of the paper channels, and that these flow rates agree with Darcy's law. The utility of these hybrid chips, for applications such as bead-, cell-, or emulsion-based assays, was demonstrated by constructing a hybrid chip that hydrodynamically focused micrometer-sized polystyrene beads stably for >10 min, as well as cells, without external instrumentation to drive fluid flow. © 2013 AIP Publishing LLC.

[<http://dx.doi.org/10.1063/1.4840575>]

### I. INTRODUCTION

Paper based microfluidics have emerged as an easy-to-use, self-contained platform to perform complex chemical and biological assays.<sup>1-5</sup> Paper microchannels use capillary forces to drive fluid flow and do not require the bulky and expensive hardware used to drive conventional microfluidics. Because these chips can operate without power or external instrumentation, they have proven particularly useful for clinical diagnostics in resource limited settings.<sup>1,6</sup> Despite its many advantages, many of the techniques developed using conventional microfluidics, such as bead,<sup>7</sup> emulsion,<sup>8</sup> and cell-based<sup>9-11</sup> assays have not been easily translated onto paper platforms.<sup>12</sup>

We herein report the development of a hybrid platform that combines conventional open-channel and paper-channel microfluidics onto a single monolithic chip (Fig. 1(a)). We fabricate our hybrid open/paper microfluidic chips using laser-micromachined plastic sheets and filter paper. On this chip, suspensions of discrete objects (i.e., cells, beads, and droplets) can be transported within conventional microfluidics that are driven and controlled by multiple paper channels. In contrast to previous works that utilized external, macroscopic paper-based pumps,<sup>13-16</sup> our work integrates paper and open channels onto a single chip. This integration

---

<sup>a)</sup> Author to whom correspondence should be addressed. Electronic mail: [Issadore@seas.upenn.edu](mailto:Issadore@seas.upenn.edu). Telephone: 215-898-5056

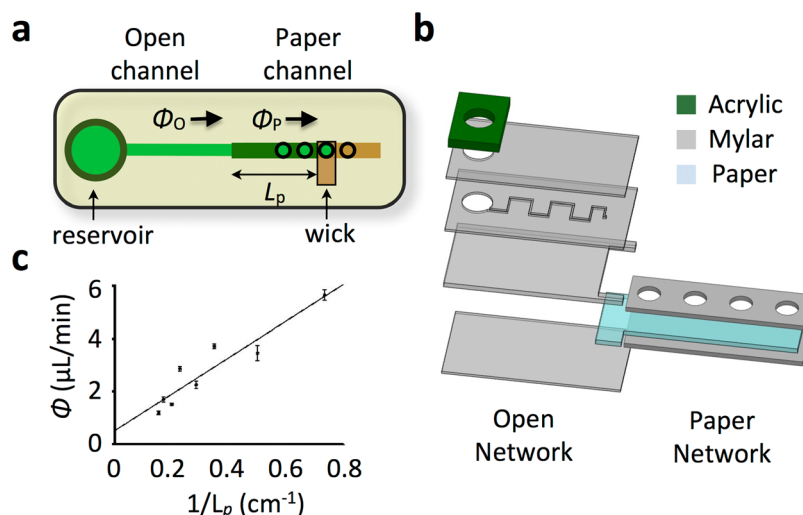


FIG. 1. Hybrid open/paper microfluidic chip harnesses the instrumentation-free advantage of paper-based platforms and extends it to conventional open-channel microfluidics. (a) Design of a simple hybrid chip. The conventional open channel is connected in series with a paper microchannel, which connects to a wick. The flow rate in the open channel  $\Phi_o$  equals the flow rate in the paper channel  $\Phi_p$ . The flow rate can be controlled by modifying the length  $L$  of the paper microchannel. (b) A prototype hybrid chip was built using layers of laser-micromachined mylar, acrylic, and filter paper. (c) Using this prototype, flow rate  $\Phi_o$  was measured as a function of the paper length  $L$ . The linear dependence of  $\Phi_o$  vs.  $1/L$  agrees with Darcy's Law ( $R^2 = 0.9958$ ).

enables the independent control of multiple open channels and control over the laminar flow-pattern within individual channels, which would require a cumbersome number of macroscopic connections using conventional methods.<sup>13–16</sup> These hybrid chips can implement complex lab-on-a-chip techniques, which require many independently controlled flow rates, on a single monolithic chip without external instrumentation to drive fluid flow. In contrast to previous works that have demonstrated the elution of cells on paper substrates,<sup>17,18</sup> our hybrid chip enables cells to be controlled using conventional microfluidic structures, such as single-cell capture sites,<sup>19</sup> inertial focusing,<sup>20</sup> and chaotic mixers.<sup>21</sup>

In this paper, we demonstrate that integrated paper microchannels can be used to quantitatively control flow in conventional microchannels. The flow rate depended linearly on the hydrodynamic resistance of the paper, in agreement with Darcy's Law. Furthermore, we show that laminar flow patterns within an open channel can be controlled using multiple paper microchannels. We demonstrate the utility of this platform by building a hybrid chip, with three paper control lines, to hydrodynamically focus polystyrene beads stably for  $>10$  min, as well as cells, in an open channel without any external instrumentation. The run-time was ultimately limited by the clogging of the paper from the polystyrene beads and could be controlled for specific applications by modifying the interfacial area between the paper and open channel.

## II. METHODS

### A. Hydrodynamic circuit model

We model the hybrid open channel/paper channel system utilizing a simple circuit model.<sup>22</sup> In this model, the flow rate  $\Phi$  is defined by the pressure difference across a channel  $\Delta P$  and its hydrodynamic resistance  $R$

$$\phi = \frac{\Delta P}{R}. \quad (1)$$

This linear relationship, Darcy's Law, is applicable because both the open channel and paper channels are low Reynolds number systems ( $\Re < 1$ ).<sup>2</sup>

We modeled an open channel that flows into a paper microchannel as two hydrodynamic resistors connected in series (Fig. 1(a)). Due to Kirchoff's current law, the flow in the open channel must equal the flow in the paper channel  $\Phi_p = \Phi_o$ . A pressure difference  $\Delta P$  is created between the fluid inlet, at atmospheric pressure, and at the wick, at a lesser pressure due to capillary action.<sup>23</sup> The hydrodynamic flow resistance of the paper, assuming that it is fully wet, is approximated by the expression<sup>2</sup>

$$R_p = \frac{\mu L_p}{\kappa w_p h_p}, \quad (2)$$

where  $\mu$  is the dynamic viscosity of the fluid,  $\kappa$  is the permeability of the paper, and  $w_p$  and  $h_p$  are the width and height of the paper microchannel. For an open channel, the flow resistance is approximated by the expression<sup>22</sup>

$$R_o = \frac{12\mu L_o}{w_o h_o^3}, \quad (3)$$

where  $w_o$  and  $h_o$  are the width and height of the open microchannel. On our chip, the paper microchannel had permeability  $\kappa \sim 10^{-12} \text{ m}^2$ ,<sup>23</sup> width  $w_p = 1 \text{ mm}$ , height  $h_p = 150 \mu\text{m}$ , and length  $L_p \sim 4 \text{ cm}$ . The open channel had a width  $w_o = 200 \mu\text{m}$ , height  $h_o = 50 \mu\text{m}$ , and length  $L_o \sim 2 \text{ cm}$ . For such a system, the resistance of the paper was much greater than that of the open channel,  $R_p/R_o \sim 100$ , and therefore changes in the geometry of the paper-microchannel lead to significant changes in the flow rate in the open channel. Furthermore, because the fluidic resistance of the paper was linearly proportional to its length  $R_p \propto L_p$ , the flow rate in the open channel  $\Phi_o \propto 1/L_p$  could be controlled by changing the length of the of the paper channel  $L_p$  (Fig. 1(a)).

## B. Fabrication

The hybrid chips were designed using SolidWorks and fabricated using a stack of laser micromachined polymer and paper sheets (Fig. 1(b)). We utilized biaxially oriented polyethylene terephthalate (BoPET) sheets, both  $50 \mu\text{m}$  thick double-sided adhesive coated (Fralock) and  $150 \mu\text{m}$  thick non-coated. The paper was Grade 1 filter paper,  $11 \mu\text{m}$  pore size (Whatman, Piscataway, NJ). The  $150 \mu\text{m}$  thick mylar layer was included to account for the difference in thickness of the paper ( $150 \mu\text{m}$ ), and the mylar layer ( $50 \mu\text{m}$ ) that defines the microchannel (Fig. 1(b)). The paper microchannels were enclosed in mylar to minimize evaporation. Kimwipe was used as a wick (Kimberly Clark, Roswell, GA). Shallow ( $3 \text{ mm}$  thick) laser-cut acrylic pieces were used as reservoirs to supply fluid at the inlets of each channel. The layers of polymer and paper sheets were cut using a  $\text{CO}_2$  laser micromachining tool (Universal Laser, VLS-2.30). The chips were assembled using a custom rig under a stereo microscope (Nikon, SMZ-1B).

## III. RESULTS

### A. Flow rate control

The control of flow rate was characterized using a simple hybrid chip design in which an open microchannel, a paper microchannel, and a wick were connected in series (Fig. 1(a)). The flow rate in the channel was controlled by moving the wick to different access points along the paper microchannel to modify its effective length  $L_p$ . The paper channel had a width  $w_p = 1 \text{ mm}$ , height  $h_p = 150 \mu\text{m}$ , and length  $L_p$  that could vary from 2 to 10 cm. The open channel had a width  $w_o = 200 \mu\text{m}$ , height  $h_o = 50 \mu\text{m}$ , and a length  $L_o = 2 \text{ cm}$ . The absolute volumetric flow rate was measured using graduations in the reservoir and a stopwatch. Initial fluid flow was driven by capillary forces within the channel. To hasten the initial fluid flow, the

plastic components of the chip were made hydrophilic by soaking them in bovine serum albumin (0.1% by weight BSA) for at least 20 min prior to assembly.

The flow-rate in the open channel could be quantitatively controlled by modifying the length of the paper microchannel  $L_p$  (Fig. 1(c)). The flow rate  $\Phi$  increased linearly with the inverse of the fluid path length  $1/L_p$ , in agreement with Darcy's law ( $R^2 = 0.9958$ ) (Eq. (2)). The measured flow rates were between 0.6 and 10  $\mu\text{l}/\text{min}$ , similar in magnitude to flow rates used in conventionally driven systems.<sup>24</sup> Longer, narrower paper microchannels would enable lower flow rates. Wider, shorter channels would enable greater flow rates. Additionally, flow rates could be increased by enlarging the interfacial area between the paper microchannel and the wick or by using a wick with greater capillary action than Kimwipes.

Efforts were taken to minimize the irregularities in flow rate in paper microchannels that arise from variations in the length and alignment of fibers.<sup>25</sup> We hypothesize that these irregularities would be small for our device because the length-scale of the fibers (pore size: 11  $\mu\text{m}$ ) was small in comparison to the microfluidic structures (channel diameter:  $w_p = 1\text{ mm}$ ). Furthermore, the orientation of the fibers in Whatman Grade 1 paper is isotropic in the plane of the paper, eliminating irregularities that arise from the orientation of the channels relative to the paper fibers.<sup>26</sup> To further reduce irregularities in flow, either larger paper channels or paper with a smaller pore size could be used.

## B. Laminar flow patterning

By integrating multiple paper control lines onto a single chip, the laminar flow pattern within an open channel could be quantitatively controlled. Control over laminar flow in open channels allows for applications such as diffusion-based assays,<sup>27</sup> the generation of chemical gradients,<sup>28</sup> and hydrodynamic focusing.<sup>9,29</sup> On our hybrid chips, we demonstrated this functionality in a conventional open channel without the typically required external instrumentation.

To demonstrate laminar flow control, we fabricated a chip with a microchannel that had a Y-junction on either end (Fig. 2(a)). The first Y-junction connected to two fluid reservoirs, one water and the other with fluorescein. The Y-junction on the output connected to two paper microchannels, each of which is connected to a wick. We varied the relative flow rate of the two output branches by controlling the lengths of the paper channels  $L_1$  and  $L_2$  (Fig. 2(a)). Fluorescence micrographs (Leica, DM4000B) of the laminar flow pattern demonstrated that the hybrid chip yields the same qualitative result obtained using two syringe pumps (NE 500, New Era Pumping Systems) to control the flow rates at the output (Fig. 2(c)). Quantitatively, the relative widths  $w_2/w_1$  of the fluorescein and water lamina show a linear dependency ( $R^2 = 0.8996$ ) on the relative channel lengths  $L_1/L_2$ , in agreement with Darcy's law (Fig. 2(b)).

## C. Flow focusing

Our hybrid design enables the transport of discrete objects, for applications such as single cell and emulsion based assays. To demonstrate this functionality, we built a flow-focusing chip and tested it with polymer beads. This type of flow focusing can be used for on-chip analysis of cells using dielectric,<sup>10</sup> magnetic,<sup>9,30</sup> and optical detection.<sup>11</sup> A flow-focusing geometry was implemented that connects to two fluid reservoirs, one containing water and the other containing a suspension of fluorescein-dyed polystyrene beads ( $d \sim 1\ \mu\text{m}$ ) (Invitrogen, Fluosphere) (Fig. 3(a)). On the output side, two paper microchannels of lengths  $L_c$  and  $L_s$  were used to control the relative flow rate of the core and sheath lamina. Fluorescence imaging (Fig. 3(b)) demonstrated that the paper microchannels could be used to control the relative width of the core and sheath lamina. By increasing the ratio  $L_s/L_c$ , the beads were focused to a narrower core.

We demonstrated that our hybrid chip could be designed to achieve stable flow of discrete objects for  $>10$  min. Discrete objects in the open channel eventually flow into the paper channel, causing the paper to clog and the flow rate to slow down accordingly. This problem can be mediated by choosing the size of the interfacial area between the paper and the open channel, such that flow is stable over a time period sufficient for a particular application. The time that a device can operate is a function of the concentration of the discrete objects, flow rate, the

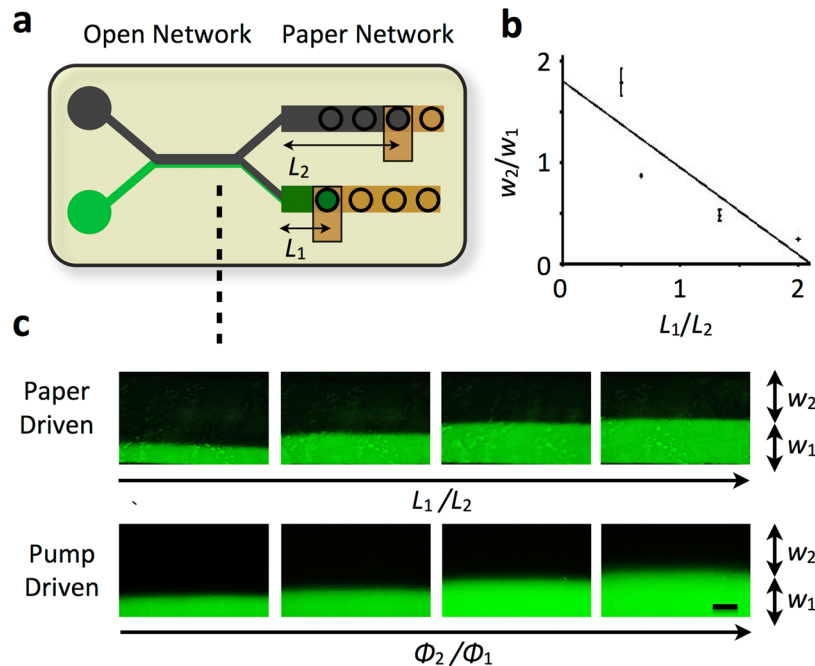


FIG. 2. Complex laminar flow patterns in a single open channel can be controlled using multiple paper microchannels. (a) A chip was fabricated with a microchannel that has a Y junction on either end, connecting to a reservoir of fluorescein and a reservoir of water on the left and paper microchannels on the right. By modifying the length  $L_1$  and  $L_2$  of the paper microchannels to the wick, the width  $w_2$  and  $w_1$  of the fluorescein-stained and the unstained lamina, respectively, can be modified. (b) The ratio  $w_2/w_1$  varies linearly with the ratio of the paper microchannel lengths  $L_1/L_2$ , in agreement with Darcy's law ( $R^2 = 0.8996$ ). (c) This trend is consistent with that observed by directly varying the ratio of the flow rates  $\Phi_2$  and  $\Phi_1$ , using syringe pumps. The scale bar is  $50 \mu\text{m}$ .

interfacial surface area, and the pore size of the paper. We designed a flow focusing hybrid chip with a  $4 \text{ mm}^2$  interface between the paper and open channel. We measured the ratio of the width of the sheath to that of the core flow  $\beta$  over time (Fig. 3(c)). A suspension of  $1 \mu\text{m}$  polystyrene beads ( $6 \times 10^6$  beads/ml) was flow focused at a flow rate of  $\sim 4 \mu\text{l}/\text{min}$ . It took  $\sim 10$  min before a significant shift ( $\Delta\beta \sim 5\%$ ) in the flow rates of the device could be observed.

To demonstrate that flow focusing can be applied to cells, cells were flow focused using a hybrid device. Cells were cultured by a collaborator, which were obtained from the pancreas of a pancreatic tumor bearing mouse (Pdx1Cre;KRAS;p53Mutant) using a collagenase digestion technique.<sup>31</sup> The cells were labeled with a nuclear mCherry that was introduced via a lentiviral infection. Fluorescence imaging (Fig. 3(d)) demonstrated that the cells could be focused to a narrower core on a hybrid chip. The sheath fluid was phosphate buffered saline (PBS) solution. The flow-focusing geometry was identical to that used in Fig. 3(b).

#### IV. DISCUSSION

We have developed a hybrid chip that integrated multiple integrated paper microchannels with open channel microfluidics to control flow in open channels on the micrometer length-scale. This approach can be used to perform conventional microfluidic assays in practical settings without the need for bulky, expensive external equipment. The platform offers the following features. (1) The system provides quantitative control of the flow rate in open channels based on the geometry of the paper channels. (2) Multiple paper control lines can be integrated onto a single chip, enabling complex laminar flow patterns within open channels to be quantitatively controlled. (3) Discrete objects, such as beads, cells, or emulsions, can be transported in the open channels stably over time scales designed for specific applications.

With such capabilities, the hybrid platform can help to translate the microfluidic tools developed using conventional microfluidics over the last decade from the laboratory into

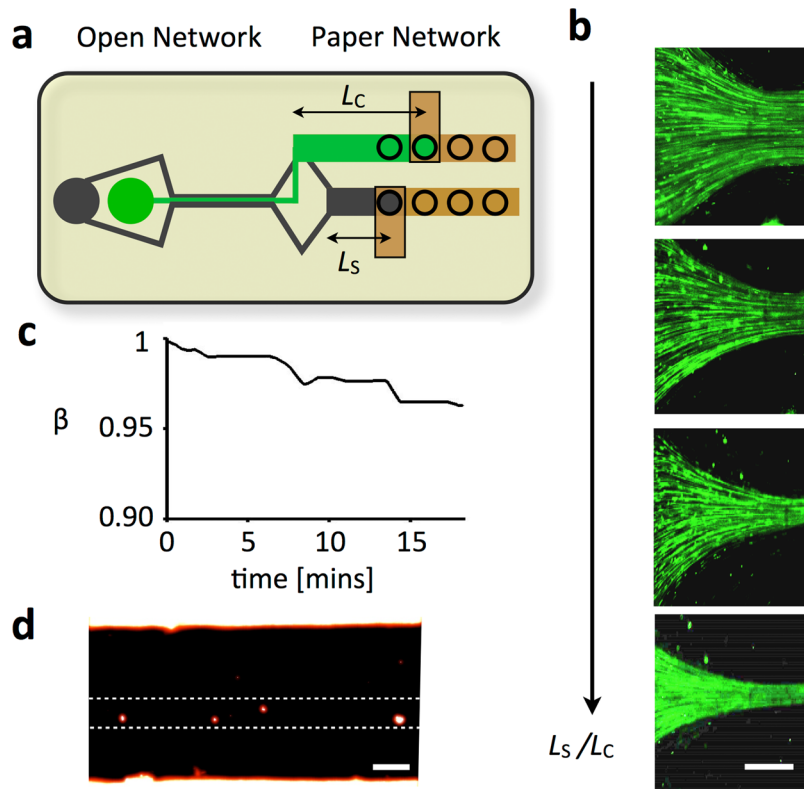


FIG. 3. Hybrid conventional channel/paper channel chips enable the instrumentation free transport of discrete objects such as beads, cells, and emulsions. (a) We fabricated a device with a flow-focusing geometry that connects to two fluid reservoirs, one containing the sheath fluid and the other containing fluorescein dyed polystyrene beads ( $d \sim 1 \mu\text{m}$ ) (Invitrogen) suspended in water. On the output side, there is a flow focusing geometry that connects to two paper microchannels of lengths  $L_c$  and  $L_s$  that each connect to a wick. (b) A series of fluorescence micrographs shows that as the ratio  $L_s/L_c$  is increased, the microbeads increasingly focused laterally towards the center of the channel. The scale bar is  $75 \mu\text{m}$ . (c) The stability of the microfluidic device was characterized by measuring the ratio of the width of the sheath to that of the core flow  $\beta$ . Over the course of 10 min, the chips showed  $\Delta\beta < 5\%$ . (d) A fluorescence micrograph showing that cells can be flow focused to a narrow stream using a hybrid conventional channel/paper channel chip. The scale bar is  $30 \mu\text{m}$ .

practical use.<sup>24</sup> The laser-cut polymer sheets and paper used in this study can be manufactured inexpensively ( $\sim 1 \text{ ¢}/\text{cm}^2$ ), enabling disposable use in resource limited settings.<sup>32</sup> Because many paper microchannels can be integrated onto a single device, applications that require complex control of flow rates in multiple channels can be implemented without the need for cumbersome pumps. Such capabilities, enables cellular, bead, or emulsion based assays developed in open-channel systems to be harnessed on these hybrid chips. For instance, flow focusing, which was demonstrate in this paper, has been used for on-chip analysis of cells using dielectric,<sup>10</sup> magnetic,<sup>9,30</sup> and optical detection.<sup>11</sup> Additionally, techniques such as single cell trapping,<sup>33</sup> and dielectrophoretic and magnetophoretic sorting,<sup>34–36</sup> which have all been designed in open-channel systems, can be implemented on these hybrid chips. Future work to further improve the hybrid platform includes utilizing recent advances in paper microfluidics that enable flow to be controlled dynamically.<sup>37</sup>

#### ACKNOWLEDGMENTS

This work was supported by the Department of Bioengineering, University of Pennsylvania, a pilot grant from the University of Pennsylvania Nano/Bio Interface Center, National Science Foundation DMR 08-32802, and a pilot grant from the University of Pennsylvania Center for AIDS Research (AI 045008). We thank Benjamin Stanger and Ravikanth Maddipati from University of Pennsylvania School of Medicine for generously providing cells for the flow focusing experiment.



- <sup>1</sup>A. W. Martinez, S. T. Phillips, G. M. Whitesides, and E. Carrilho, "Diagnostics for the developing world: Microfluidic paper-based analytical devices," *Anal. Chem.* **82**, 3–10 (2010).
- <sup>2</sup>J. L. Osborn, B. Lutz, E. Fu, P. Kauffman, D. Y. Stevens, and P. Yager, "Microfluidics without pumps: Reinventing the T-sensor and H-filter in paper networks," *Lab Chip* **10**, 2659–2665 (2010).
- <sup>3</sup>Y. Lu, W. Shi, J. Qin, and B. Lin, "Fabrication and characterization of paper-based microfluidics prepared in nitrocellulose membrane by wax printing," *Anal. Chem.* **82**, 329–335 (2010).
- <sup>4</sup>S. A. Klasner, A. K. Price, K. W. Hoeman, R. S. Wilson, K. J. Bell, and C. T. Culbertson, "Paper-based microfluidic devices for analysis of clinically relevant analytes present in urine and saliva," *Anal. Bioanal. Chem.* **397**, 1821–1829 (2010).
- <sup>5</sup>X. Li, D. R. Ballerini, and W. Shen, "A perspective on paper-based microfluidics: Current status and future trends," *Biomicrofluidics* **6**, 011301 (2012).
- <sup>6</sup>F. A. Gomez, "The future of microfluidic point-of-care diagnostic devices," *Bioanalysis* **5**, 1–3 (2013).
- <sup>7</sup>K.-Y. Lien, L.-Y. Hung, T.-B. Huang, Y.-C. Tsai, H.-Y. Lei, and G.-B. Lee, "Rapid detection of influenza A virus infection utilizing an immunomagnetic bead-based microfluidic system," *Biosens. Bioelectron.* **26**, 3900–3907 (2011).
- <sup>8</sup>H. Zhang, S. Nie, C. M. Etsen, R. M. Wang, and D. R. Walt, "Oil-sealed femtoliter fiber-optic arrays for single molecule analysis," *Lab Chip* **12**, 2229–2239 (2012).
- <sup>9</sup>D. Issadore, J. Chung, H. Shao, M. Liong, A. A. Ghazani, C. M. Castro, R. Weissleder, and H. Lee, "Ultrasensitive clinical enumeration of rare cells *ex vivo* using a micro-hall detector," *Sci. Transl. Med.* **4**, 141ra92 (2012).
- <sup>10</sup>D. K. Wood, S.-H. Oh, S.-H. Lee, H. T. Soh, and A. N. Cleland, "High-bandwidth radio frequency Coulter counter," *Appl. Phys. Lett.* **87**, 184106 (2005).
- <sup>11</sup>O. Schmidt, M. Bassler, P. Kiesel, C. Knollenberg, and N. Johnson, "Fluorescence spectrometer-on-a-fluidic-chip," *Lab Chip* **7**, 626–629 (2007).
- <sup>12</sup>D. D. Liana, B. Raguse, J. J. Gooding, and E. Chow, "Recent advances in paper-based sensors," *Sensors* **12**, 11505–11526 (2012).
- <sup>13</sup>X. Wang, J. A. Hagen, and I. Papautsky, "Paper pump for passive and programmable transport," *Biomicrofluidics* **7**, 014107 (2013).
- <sup>14</sup>Z.-R. Xu, C.-H. Zhong, Y.-X. Guan, X.-W. Chen, J.-H. Wang, and Z.-L. Fang, "A microfluidic flow injection system for DNA assay with fluids driven by an on-chip integrated pump based on capillary and evaporation effects," *Lab Chip* **8**, 1658–1663 (2008).
- <sup>15</sup>J. Wang, H. Ahmad, C. Ma, Q. Shi, O. Vermesh, U. Vermesh, and J. Heath, "A self-powered, one-step chip for rapid, quantitative, and multiplexed detection of proteins from pinpricks of whole blood," *Lab Chip* **10**, 3157–3162 (2010).
- <sup>16</sup>P. K. Yuen, "Fluid control in microfluidic devices using a fluid conveyance extension and an absorbent microfluidic flow modulator," *Lab Chip* **13**, 1737–1742 (2013).
- <sup>17</sup>L. Li, J. Tian, D. Ballerini, M. Li, and W. Shen, "A study of the transport and immobilisation mechanisms of human red blood cells in a paper-based blood typing device using confocal microscopy," *Analyst* **138**, 4933–4940 (2013).
- <sup>18</sup>M. Al-Tamimi, W. Shen, R. Zeineddine, H. Tran, and G. Garnier, "Validation of paper-based assay for rapid blood typing," *Anal. Chem.* **84**, 1661–1668 (2012).
- <sup>19</sup>J. Chung, D. Issadore, A. Ullal, K. Lee, R. Weissleder, and H. Lee, "Rare cell isolation and profiling on a hybrid magnetic/size-sorting chip," *Biomicrofluidics* **7**, 054107 (2013).
- <sup>20</sup>D. Di Carlo, "Inertial microfluidics," *Lab Chip* **9**, 3038–3046 (2009).
- <sup>21</sup>A. D. Stroock, S. K. W. Dertinger, A. Ajdari, M. Igor, H. A. Stone, and G. M. Whitesides, "Chaotic mixer for microchannels," *Science* **295**, 647–651 (2002).
- <sup>22</sup>H. Lee, D. Ham, and R. M. Westervelt, *CMOS Biotechnology* (Springer, 2007).
- <sup>23</sup>E. Fu, S. A. Ramsey, P. Kauffman, B. Lutz, and P. Yager, "Transport in two-dimensional paper networks," *Microfluid. Nanofluid.* **10**, 29–35 (2011).
- <sup>24</sup>D. Issadore and R. Westervelt, *Point-of-Care Diagnostics on a Chip* (Springer, 2013).
- <sup>25</sup>A. R. Rezk, A. Qi, J. R. Friend, W. H. Li, and L. Y. Yeo, "Uniform mixing in paper-based microfluidic systems using surface acoustic waves," *Lab Chip* **12**, 773–779 (2012).
- <sup>26</sup>A. W. Martinez, S. T. Phillips, B. J. Wiley, M. Gupta, and G. M. Whitesides, "FLASH: A rapid method for prototyping paper-based microfluidic devices," *Lab Chip* **8**, 2146–2150 (2008).
- <sup>27</sup>A. Hatch, A. E. Kamholz, K. R. Hawkins, M. S. Munson, E. A. Schilling, B. H. Weigl, and P. Yager, "A rapid diffusion immunoassay in a T-sensor," *Nat. Biotechnol.* **19**, 461–465 (2001).
- <sup>28</sup>N. L. Jeon, S. K. W. Dertinger, D. T. Chiu, I. S. Choi, A. D. Stroock, and G. M. Whitesides, "Generation of solution and surface gradients using microfluidic systems," *Langmuir* **16**, 8311–8316 (2000).
- <sup>29</sup>M. Rosenauer, W. Buchegger, I. Finoulst, P. Verhaert, and M. Vellekoop, "Miniaturized flow cytometer with 3D hydrodynamic particle focusing and integrated optical elements applying silicon photodiodes," *Microfluid. Nanofluid.* **10**, 761–771 (2011).
- <sup>30</sup>D. Issadore, H. J. Chung, J. Chung, G. Budin, R. Weissleder, and H. Lee, "μHall chip for sensitive detection of bacteria," *Adv. Healthcare Mater.* **2**, 1224–1228 (2013).
- <sup>31</sup>A. D. Rhim, E. T. Mirek, N. M. Aiello, A. Maitra, J. M. Bailey, F. McAllister, M. Reichert, G. L. Beatty, A. K. Rustgi, R. H. Vonderheide *et al.*, "EMT and dissemination precede pancreatic tumor formation," *Cell* **148**, 349–361 (2012).
- <sup>32</sup>A. W. Martinez, S. T. Phillips, and G. M. Whitesides, "Three-dimensional microfluidic devices fabricated in layered paper and tape," *Proc. Natl. Acad. Sci. U.S.A.* **105**, 19606–19611 (2008).
- <sup>33</sup>D. Di Carlo, L. Y. Wu, and L. P. Lee, "Dynamic single cell culture array," *Lab Chip* **6**, 1445–1449 (2006).
- <sup>34</sup>K. Ahn, C. Kerbage, T. P. Hunt, R. M. Westervelt, D. R. Link, and D. A. Weitz, "Dielectrophoretic manipulation of drops for high-speed microfluidic sorting devices," *Appl. Phys. Lett.* **88**, 024104–024104 (2006).
- <sup>35</sup>D. Issadore, T. Franke, K. A. Brown, T. P. Hunt, and R. M. Westervelt, "High-voltage dielectrophoretic and magnetophoretic hybrid integrated circuit/microfluidic chip," *J. Microelectromech. Syst.* **18**, 1220–1225 (2009).
- <sup>36</sup>J. D. Adams, U. Kim, and H. T. Soh, "Multitarget magnetic activated cell sorter," *Proc. Natl. Acad. Sci. U.S.A.* **105**, 18165–18170 (2008).
- <sup>37</sup>B. Lutz, T. Liang, E. Fu, S. Ramachandran, P. Kauffman, and P. Yager, "Dissolvable fluidic time delays for programming multi-step assays in paper diagnostics," *Lab Chip* **13**, 2840–2847 (2013).